Geomechanics and Engineering, *Vol. 10, No. 2 (2016) 175-188*
DOI: http://dx.doi.org/10.12989/gae.2016.10.2.175

Predictive models of ultimate and serviceability performances for underground twin caverns

Wengang Zhang [1,2,3] and Anthony T.C. Goh [*3]

[1] *Key Laboratory of New Technology for Construction of Cities in Mountain Area (Chongqing University), Ministry of Education, Chongqing 400045, China*
[2] *School of Civil Engineering, Chongqing University, Chongqing 400045, China*
[3] *School of Civil and Environmental Engineering, Nanyang Technological University, 639798 Singapore*

(*Received December 12, 2014, Revised December 03, 2015, Accepted December 08, 2015*)

Abstract. The construction of a new cavern modifies the state of stresses and displacements in a zone around the existing cavern. For multiple caverns, the size of this influence zone depends on the ground type, the in situ stress, the cavern span and shape, the width of the pillar separating the caverns, and the excavation sequence. Performances of underground twin caverns can be unsatisfactory as a result of either instability (collapse) or excessive displacements. These two distinct failures should be prevented in design. This study simulated the ultimate and serviceability performances of underground twin rock caverns of various sizes and shapes. The global factor of safety is used as the criterion for determining the ultimate limit state and the calculated maximum displacement around the cavern opening is adopted as the serviceability limit state criterion. Based on the results of a series of numerical simulations, simple regression models were developed for estimating the global factor of safety and the maximum displacement, respectively. It was proposed that a proper pillar width can be determined based on the threshold influence factor value. In addition, design charts with regard to the selection of the pillar width for underground twin rock caverns under similar ground conditions were also developed.

Keywords: influence factor; ultimate and serviceability performances; pillar width; global factor of safety; maximum displacement

1. Introduction

Nowadays, multiple excavations are used for many applications such as: subways, hydraulic tunnels, railways, and storage caverns. For multiple caverns, the construction of a new cavern in close proximity to an existing cavern modifies the state of stresses and movements in a zone around the existing cavern. Usually, the size of this influence zone depends on the ground type, the in situ stress, the cavern span and shape, the width of the pillar separating the caverns, and the excavation sequence. This interaction between close excavations were intensively investigated based on field measurements and analytical methods (e.g., Barla and Ottoviani 1974, Ghaboussi and Ranken 1977, Gercek 2005, Zhao and Ma 2009, Mortazavi *et al*. 2009, Karademir 2010, Esterhuizen *et al*. 2011, Li *et al*. 2012, Jiao *et al*. 2013a, b, 2015).

∗Corresponding author, Associate Professor, E-mail: ctcgoh@ntu.edu.sg

http://www.techno-press.org/?journal=gae&subpage=7 ISSN: 2005-307X (Print), 2092-6219 (Online)

Conventional evaluation of stability of geotechnical structures and underground openings involves determining the relationship between the resistance and the load or calculating the induced displacements/strains. The former is usually used as the criterion for assessing the ultimate limit state while the latter is adopted as the serviceability limit state criterion. However, it must be noted that, for underground caverns, neither the factor of safety *FS* nor the induced displacement is known explicitly. Instead, it may be determined only through repeated point-by-point numerical analyses with different design parameters. Generally, the performance function is constructed artificially using polynomial or logarithmic regression methods (e.g., Basarir 2008, Zhu *et al*. 2008, Goh and Zhang 2012, Zhang and Goh 2012, Siahmansouri *et al*. 2012). Alternatively, the Multivariate adaptive regression splines (MARS) algorithm and the Artificial Neural Network approach (ANN) are also used to develop surrogate response surface models (Goh and Zhang 2012, Lü *et al*. 2012, Mahdevari and Torabi 2012, Rafiai and Moosavi 2012, Zhang and Goh 2013, Adoko *et al*. 2013). Though slightly inferior to the MARS and ANN methods in terms of predictive accuracy, the regression models remain popular due to its simplicity and model interpretability.

This paper describes a parametric study to investigate the ultimate and serviceability performances of underground twin rock caverns. The global factor of safety obtained using the shear strength reduction technique is used as the criterion for determining the ultimate limit state and the calculated maximum displacement around the opening is adopted as the serviceability limit state criterion. Based on the numerical results, regression models were developed for estimating the global factor of safety and the induced maximum displacement, respectively. An Influence Factor which is defined as the ratio of the induced displacement of the existing cavern as a result of excavation of the second opening to value of the single cavern case is proposed in this study. A proper pillar width can be determined based on the threshold Influence Factor value.

2. Methodologies

2.1 Rock mass classifications

When performing numerical analysis, the selection of appropriate input parameters, especially in the preliminary stage of an engineering design, is essential. Various indirect empirical relations have been proposed to calculate the rock mass properties such as the deformation modulus E_m, the shear strength indices c and ϕ and the rock uniaxial compressive strength σ_{cm}. For the numerical analyses that were carried out, the following equations (Eqs. (1)-(7)) were adopted for determining the rock mass properties.

$$RMR = 7lnQ + 3 \qquad \text{(Tugrul 1998)} \tag{1}$$

$$E_m(GPa) = 10^{(RMR-10)/40} \ (RMR \leq 50) \qquad \text{(Serafim and Pereira 1983)} \tag{2}$$

$$E_m(GPa) = 2RMR - 100 \ (RMR > 50) \qquad \text{(Bieniawski 1978)} \tag{3}$$

$$c(MPa) = 0.005(RMR - 1) \qquad \text{(Bieniawski 1989)} \tag{4}$$

$$\phi(^\circ) = 0.5RMR + 4.5 \qquad \text{(Bieniawski 1989)} \tag{5}$$

Table 1 Rock mass properties with different Q values

Q	c (MPa)	ϕ (°)	E_m (GPa)	μ	σ_t (MPa)
10	0.26	30.6	11.3	0.20	3.47
40	0.30	35.4	19.7	0.16	4.12
100	0.34	38.6	28.6	0.16	4.55

$$\sigma_{cm}\,(MPa) = RMR \qquad \text{(Palmstrom 2000)} \tag{6}$$

$$\sigma_t(MPa) = \sigma_{cm}/15 \tag{7}$$

where E_m is the deformation modulus of rock mass, c is the cohesive strength, ϕ is the friction angle, σ_{cm} is the uniaxial compressive strength (*UCS*) and σ_t is the tensile strength. Adopting the above empirical equations, the Q value of each category to be considered in this study and its corresponding rock properties are shown in Table 1. In Table 1, the Poisson's ratio μ values are assumed. For simplicity, density of 2670 kg/m^3 is assumed for rock mass for all the ranges of Q. It should always be noted that these relationships are intended to provide the initial estimates of the rock mass properties and should be used with great caution in engineering design.

2.2 Shear strength reduction technique

In this study, the global stability FS_{gt} values are assessed using the shear strength reduction technique (SSR). This technique has been used by various authors including Matsui and San (1992), Dawson *et al*. (1999, 2000), and is now available in many commercial finite element (FEM) and finite difference (FDM) programs. This procedure essentially involves repeated analyses by progressively reducing the shear strength properties until collapse occurs. For a Mohr-Coulomb material, by reducing the shear strength by a factor F the shear strength equation becomes

$$\frac{\tau_f}{F} = \frac{c}{F} + \sigma_n \frac{tan\phi}{F} \tag{8}$$

$$F = \frac{\tau_f}{c^* + \sigma_n tan\phi^*} \tag{9}$$

where τ_f is the shear strength, σ_n is the normal stress, and $c^* = c/F$ and $\phi^* = arc\tan(\tan\phi/F)$ are the new Mohr-Coulomb shear strength parameters. Systematic increments of F are performed until the finite element or finite difference model does not converge to a solution (i.e. failure occurs). The critical strength reduction value which corresponds to non-convergence is taken to be the global factor of safety *FS*. The technique has been applied to a number of underground excavation problems including rock caverns (Hammah *et al*. 2007, Zhang and Goh 2012, Goh and Zhang 2012) and circular tunnels (Vermeer *et al*. 2002).

3. Numerical models and modeling results

The FDM FLAC3D code (Itasca 2005) was utilized for the numerical experiments, even though only plane strain analyses were carried out, as future studies will consider the 3D effects.

3.1 Assumptions of numerical analysis

The basic assumptions of numerical analyses and the cross section layout of the twin caverns are:

(a) the study was a two-dimensional plane strain problem;
(b) *Q* cannot be directly used in the FLAC^{3D} calculations, though it is a commonly used quality index representing rock mass competence. Thus the discontinuous nature of the rock is incorporated implicitly in the Mohr-Coulomb constitutive relationship used to represent the mass as an equivalent continuum;
(c) the rock material obeyed Mohr-Coulomb failure criterion that follows the elastic perfectly-plastic stress-strain relationship;
(d) the caverns are unsupported;
(e) the twin caverns are of equal size, both horse-shoe shaped, with semi-circular roof, and horizontally aligned;
(f) the excavation involves two stages: excavation of the first cavern, followed by the second cavern, both full-face excavation;
(g) the effect of creep was not considered in the analysis.

3.2 Cross-section layout

One significant parameter influencing the interaction is the cavern span *B*. In this study, cavern span values of 10, 20 and 30 m are considered. In the numerical models, the cavern crown is 65 m below the ground surface. The initial vertical in situ stress σ_v is induced by self-weight of the rock. The horizontal stress σ_h is calculated using $K_0 \times \sigma_v$. The physical and geometrical model including the twin caverns and the design variables considered are shown in Fig. 1. The plane strain conditions are enforced by including a thin 1 m slice of material in the longitudinal direction and imposing boundary conditions on the two off-plane surfaces that allow movement vertically but are restrained against displacements normal to these planes. Outer boundaries are located far from the cavern to minimize the boundary effects. No surface loading above ground surface is considered. The two dependent responses are the global factor of safety FS_{gt} and the maximum

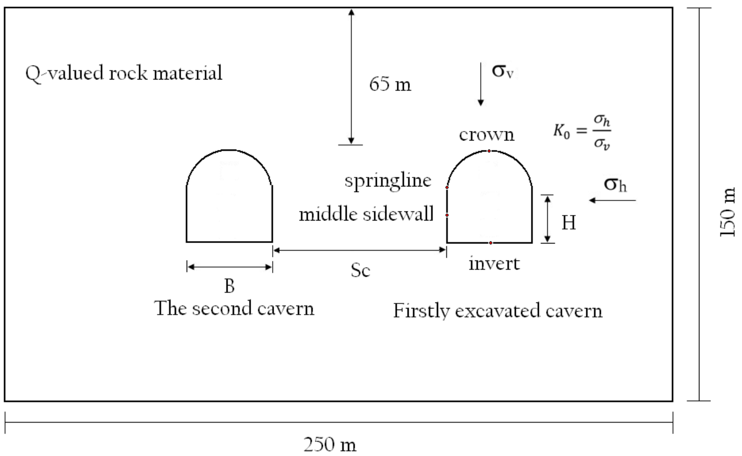

Fig. 1 Geometrical model and basic design parameters

displacement $u_{\max}$. The former is calculated by the shear strength reduction technique, in which the shear strengths are systematically reduced until failure occurs while the latter is the maximum displacements of key points including crown *C*, springline *S*, middle sidewall *M*, and invert *I* induced during the excavation process, as illustrated in Fig. 1.

3.3 Ranges of design parameters

The main factors affecting twin cavern performances are found to be the cavern geometrical characteristics, the rock strength properties, the in situ stress field, and the excavation sequence. The important design parameters mentioned above are shown in Table 2. Since only unsupported caverns are considered in this study only, Q values of 10, 40, and 100 are considered, as values of Q lower than 10 would not be able to stand unsupported for these cavern geometries.

3.4 Modeling results of FS_{gt}

The FS_{gt} values are summarized in Table 3.

Table 2 Factors and their values used

Parameter	Description	Values
K_0	In situ stress ratio	0.5, 1, 2
B	Cavern span (m)	10, 20, 30
S_c/B	Ratio of pillar width to cavern span	1, 1.5, 2, 2.5
Q	Tunneling quality index	10, 40, 100
B/H	Cavern shape	1, 2, 4

Table 3 Results from numerical experiments for FS_{gt}

B/H	B (m)	Q	FS_{gt}			
			S_c/B = 1	S_c/B = 1.5	S_c/B = 2	S_c/B = 2.5
1	10	10	1.44	1.44	1.45	1.47
		40	1.71	1.71	1.72	1.75
		100	1.91	1.93	1.94	1.96
	20	10	1.01	1.05	1.10	1.16
		40	1.20	1.24	1.31	1.38
		100	1.35	1.40	1.47	1.54
	30	10	0.85	0.89	0.97	1.06
		40	1.01	1.06	1.17	1.25
		100	1.12	1.19	1.30	1.40
2	10	10	1.61	1.62	1.65	1.68
		40	1.90	1.92	1.96	2.00
		100	2.13	2.15	2.20	2.24
	20	10	1.17	1.23	1.29	1.35
		40	1.38	1.46	1.53	1.61
		100	1.55	1.64	1.72	1.79

Table 3 Continued

B/H	B (m)	Q	FS_{gt}			
			S_c/B = 1	S_c/B = 1.5	S_c/B = 2	S_c/B = 2.5
	30	10	1.04	1.10	1.19	1.25
		40	1.24	1.31	1.42	1.48
		100	1.38	1.47	1.59	1.66
4	10	10	1.71	1.74	1.78	1.81
		40	2.03	2.07	2.11	2.15
		100	2.27	2.32	2.37	2.41
	20	10	1.26	1.34	1.41	1.47
		40	1.49	1.59	1.67	1.75
		100	1.67	1.78	1.87	1.96
	30	10	1.15	1.22	1.30	1.31
		40	1.36	1.45	1.54	1.56
		100	1.52	1.62	1.73	1.74

Fig. 2 shows that for the same Q and B, FS_{gt} increases with the S_c/B and B/H ratios.

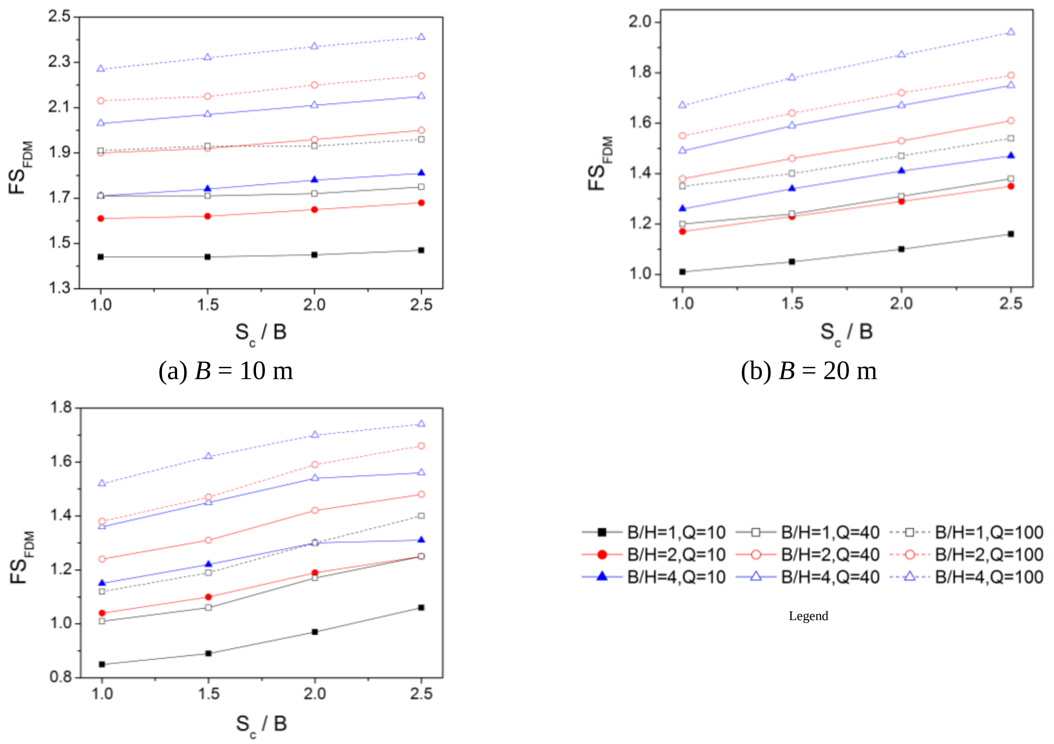

(a) B = 10 m

(b) B = 20 m

(c) B = 30 m

Fig. 2 Influences of S_c and B/H on FS_{gt}

3.5 Modeling results of u_{max}

u_{max} values are calculated except for the cases with $FS_{gt} < 1$. A total of 315 cases are analyzed and the results are shown in Table 4.

Fig. 3 shows the influences of design parameters on u_{max}. It is obvious that generally with increase of S_c/B, u_{max} converges. u_{max} decreases as Q increases since higher Q corresponds to greater deformation modulus and increased strength of the rock mass. In addition, for the same Q value, u_{max} is significantly influenced by K_0.

Table 4 Results from numerical experiments for u_{max}

B/H	B (m)	Q	u_{max} (mm)											
			$S_c/B = 1$			$S_c/B = 1.5$			$S_c/B = 2$			$S_c/B = 2.5$		
			$K_0 = 0.5$	1	2	0.5	1	2	0.5	1	2	0.5	1	2
1	10	10	6.14	5.63	9.59	5.87	5.49	8.93	3.8	4.23	8.61	3.11	4.09	8.53
		40	2.20	2.02	4.22	1.61	1.84	4.21	1.52	1.82	4.19	1.47	1.78	4.07
		100	1.16	1.13	2.68	1.02	1.12	2.67	0.97	1.10	2.66	0.94	1.08	2.55
	20	10	74.31	17.19	31.82	27.25	13.77	19.8	13.28	11.39	17.90	8.71	9.41	16.76
		40	6.46	6.15	8.69	4.02	4.08	8.22	3.31	3.94	8.10	3.06	3.83	7.95
		100	2.98	2.71	5.44	2.05	2.39	5.29	1.90	2.34	5.24	1.86	2.28	5.15
	30	10	—	—	—	—	—	—	—	—	—	18.64	18.06	23.62
		40	72.27	12.48	12.9	10.3	8.80	11.89	5.94	6.05	10.64	5.30	5.74	10.03
		100	5.73	4.88	7.23	3.68	3.60	7.18	3.18	3.42	6.83	2.93	3.26	6.51
2	10	10	3.77	3.12	6.10	2.59	2.68	5.96	2.50	2.57	5.87	2.43	2.49	5.79
		40	1.40	1.31	2.76	1.31	1.23	2.74	1.27	1.18	2.73	1.25	1.15	2.69
		100	0.90	0.83	1.72	0.86	0.78	1.71	0.83	0.76	1.70	0.82	0.74	1.68
	20	10	12.88	11.5	13.25	6.63	6.12	11.8	5.71	5.69	11.43	5.34	5.48	11.20
		40	3.14	2.73	5.50	2.64	2.57	5.45	2.52	2.51	5.39	2.48	2.46	5.26
		100	1.78	1.67	3.44	1.67	1.61	3.41	1.64	1.57	3.35	1.63	1.54	3.28
	30	10	37.88	16.55	17.92	11.19	9.84	15.76	8.97	8.64	15.58	8.22	8.08	15.28
		40	4.65	3.93	7.19	4.10	3.61	7.13	3.74	3.48	6.86	3.54	3.44	6.52
		100	2.65	2.31	4.84	2.43	2.27	4.5	2.35	2.23	4.33	2.34	2.20	4.13
4	10	10	2.43	2.34	5.05	2.28	2.23	4.96	2.21	2.16	4.83	2.16	2.10	4.72
		40	1.24	1.14	2.06	1.19	1.10	2.03	1.16	1.05	1.99	1.13	1.03	1.94
		100	0.81	0.75	1.25	0.78	0.72	1.23	0.76	0.70	1.21	0.75	0.69	1.18
	20	10	6.23	5.47	10.02	5.03	4.83	9.86	4.67	4.61	9.72	4.45	4.46	9.60
		40	2.51	2.30	4.16	2.31	2.25	4.08	2.28	2.19	3.98	2.27	2.17	3.87
		100	1.58	1.50	2.56	1.54	1.46	2.50	1.52	1.43	2.43	1.50	1.40	2.38
	30	10	9.39	7.94	12.78	7.79	7.36	12.56	7.02	6.78	12.47	6.61	6.39	12.22
		40	3.70	3.19	5.23	3.43	3.10	5.13	3.21	3.06	5.07	3.17	3.00	4.89
		100	2.26	2.10	3.24	2.16	2.06	3.18	2.14	2.04	3.14	2.13	2.01	2.99

S_c/B S_c/B S_c/B

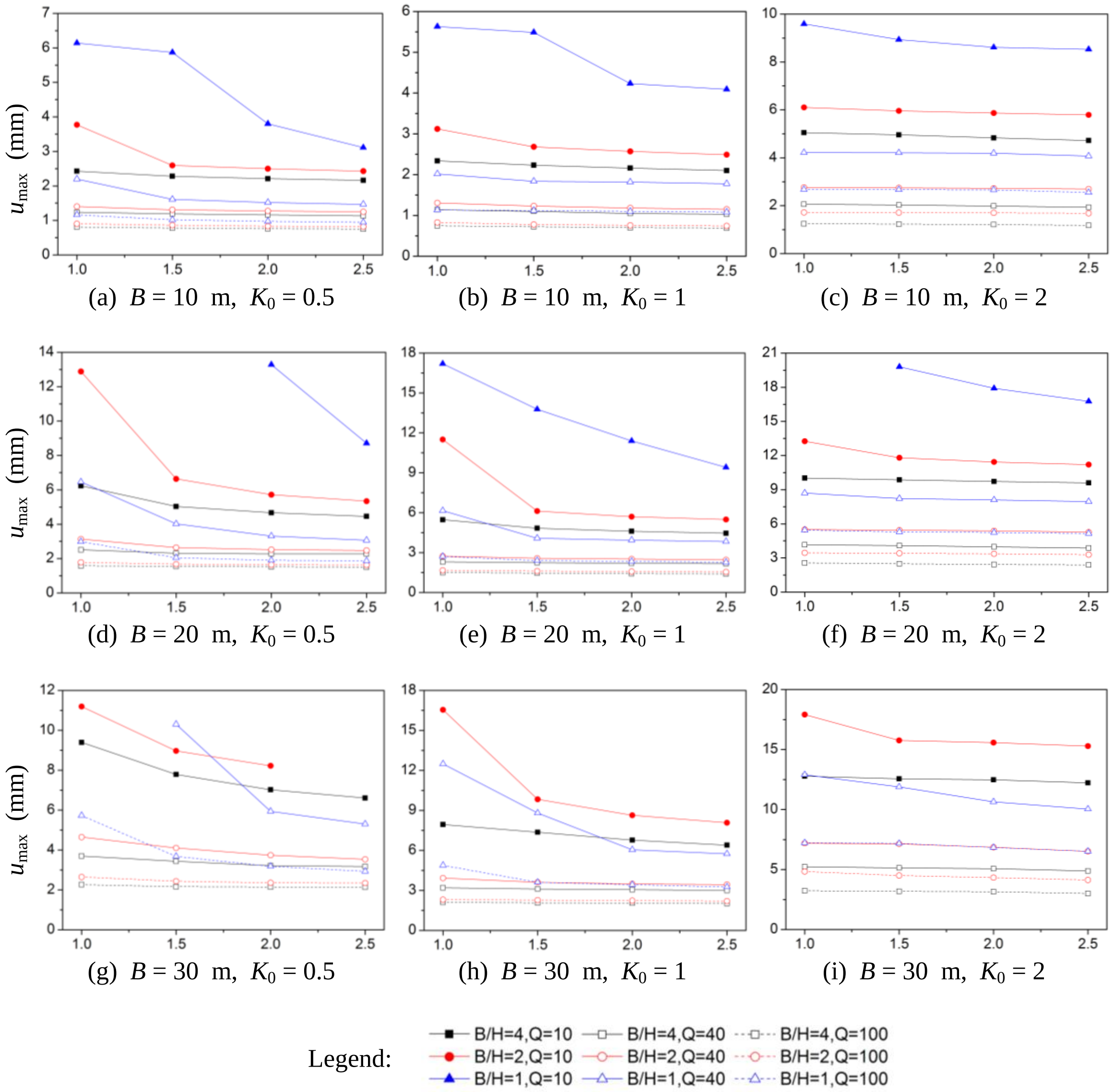

(a) $B = 10$ m, $K_0 = 0.5$ (b) $B = 10$ m, $K_0 = 1$ (c) $B = 10$ m, $K_0 = 2$

(d) $B = 20$ m, $K_0 = 0.5$ (e) $B = 20$ m, $K_0 = 1$ (f) $B = 20$ m, $K_0 = 2$

(g) $B = 30$ m, $K_0 = 0.5$ (h) $B = 30$ m, $K_0 = 1$ (i) $B = 30$ m, $K_0 = 2$

Fig. 3 Influences of S_c, Q, K_0, B and B/H on u_{max}

4. Regression models

4.1 Regression model for FS_{gt}

Based on Table 3, the Logarithmic Regression (LR) model was developed for predicting FS_{gt} in terms of Q, B, S_c/B and B/H, as shown in Eq. (10)

$$FS_{gt_{LR}} = 2.2433(B/H)^{0.1702} B^{-0.3515} Q^{0.1239} (S_c/B)^{0.1345} \tag{10}$$

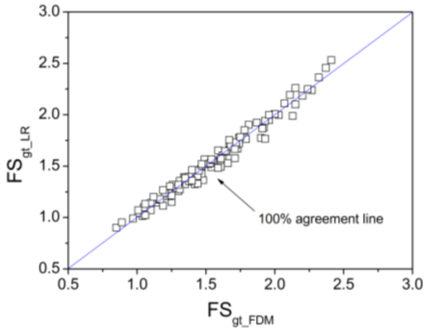

Fig. 4 Comparison between FS_{gt_FDM} and FS_{gt_LR}

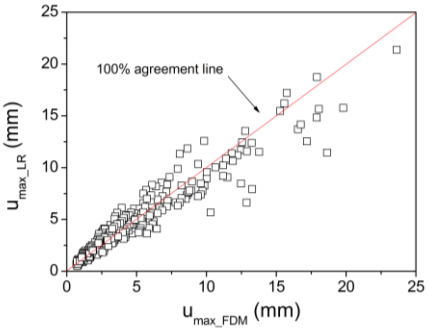

Fig. 5 Comparison between $u_{\max\_\mathrm{FDM}}$ and $u_{\max\_\mathrm{LR}}$

A comparison between FS_{gt_LR} and FS_{gt_FDM} (the global factor of safety obtained from FLAC^{3D}) is shown in Fig. 4. The high coefficient of determination R^2 of 0.923 indicates that the LR predictions are in good agreement with the target FDM FS_{gt} values.

4.2 Regression model for $u_{\max}$

The LR model developed for predicting $u_{\max}$ in terms of Q, B, B/H, S_c/B and K_0 is shown below

$$u_{\max}\,(mm) = 2.2725(B/H)^{-0.4675}B^{1.0163}Q^{-0.5805}(K_0)^{0.4513}(S_c/B)^{-0.2078} \tag{11}$$

A plot of $u_{\max\_LR}$ versus $u_{\max\_\mathrm{FDM}}$ shown in Fig. 5 with R^2 = 0.909 indicates that the *LR* predictions are generally in agreement with the target FDM $u_{\max}$, particularly for $u_{\max}$ less than 10 mm. It should be noted that in developing the LR model, only cases with $u_{\max}$ less than 25 mm are considered in Eq. (11) since with larger values of $u_{\max}$ it is unlikely that the serviceability limit state would be satisfactory.

5. Influence factor

To address the influences of the excavation of the second cavern on the existing opening, a term of Influence Factor (λ_{ut}) is introduced, as defined in Eq. (12)

Table 5 Results from numerical experiments for $u_{\text{max\_single}}$ (mm)

B/H	B (m)	Q = 10			Q = 40			Q = 100		
		K_0 = 0.5	K_0 = 1	K_0 = 2	K_0 = 0.5	K_0 = 1	K_0 = 2	K_0 = 0.5	K_0 = 1	K_0 = 2
4	10	2.17	2.22	5.26	1.14	1.06	1.99	0.76	0.69	1.21
	20	4.39	4.44	10.53	2.34	2.20	3.98	1.56	1.43	2.36
	30	6.43	6.40	14.56	3.46	3.26	5.77	2.32	2.15	3.35
2	10	2.40	2.54	6.19	1.24	1.16	2.65	0.82	0.74	1.63
	20	4.92	5.26	12.56	2.58	2.47	5.21	1.71	1.57	3.23
	30	7.31	7.68	17.71	3.90	3.73	7.35	2.59	2.39	4.60
1	10	2.87	3.55	8.26	1.42	1.60	3.98	0.92	1.00	2.48
	20	5.97	8.05	16.99	3.06	3.50	7.93	1.99	2.15	5.05
	30	11.10	13.65	24.88	4.64	5.51	11.30	3.04	3.30	7.30

$$\lambda_{ut}\,(\%) = \frac{u_{\max} - u_{\substack{\max \\ single}}}{u_{\substack{\max \\ single}}} \times 100 \tag{12}$$

in which $u_{\max}$ has been defined as in Sections 3.5 and 4.2; $u_{\text{max\_single}}$ is the maximum displacement of the existing opening before the excavation of the second cavern. The $u_{\text{max\_single}}$ values are listed in Table 5. Based on Tables 4 and 5, the λ_{ut} value for each case can be determined

The *LR* models developed for predicting λ_{ut} in terms of Q, B, B/H, and S_c/B for K_0 = 0.5, 1, and 2 are shown below

$$\lambda_{ut}\,(\%) = 307.45(B/H)^{-1.610}B^{0.663}Q^{-0.779}(S_c/B)^{-3.303} \qquad K_0 = 0.5 \tag{13a}$$

$$\lambda_{ut}\,(\%) = 407.57(B/H)^{-1.475}B^{0.046}Q^{-0.510}(S_c/B)^{-3.012} \qquad K_0 = 1 \tag{13b}$$

$$\lambda_{ut}\,(\%) = 9.893(B/H)^{-0.629}B^{0.146}Q^{-0.078}(S_c/B)^{-2.562} \qquad K_0 = 22 \tag{13c}$$

It should be noted that for Eqs. (10), (11) and (13), the coefficients are determined by the method of least squares, which minimizes the sum of squared deviations between the fitted and actual data.

6. Design charts of λ_{ut} and determination of S_c/B

The interaction of the excavation of the second cavern on the existing opening has great importance during the preliminary design phase, particularly when the plan and profile of the twin caverns are under design consideration. As a result, introducing simple predictive model or design charts to determine a proper pillar width is essential for decision making. Furthermore precise assessment of the global factor of safety or the induced deformations should be conducted to assure the stability and serviceability performances during construction.

It is proposed in this study that some certain threshold λ_{ut} value, i.e., 10 or 20, be used to limit the deformation induced as a result of excavation of the adjacent cavern. During construction, if the measured displacement is within the acceptable level, then excavation continues. Otherwise, a greater pillar width or additional supports should be required. Based on Eq. (13), a series of design charts are developed, as illustrated in Fig. 6, assuming threshold λ_{ut} values of 10 and 20.

Based on Eq. (13) and Fig. 6, a S_c/B ratio no less than the values proposed in Table 6 can be used to limit the displacement of the existing opening induced by excavation of adjacent cavern within acceptable range. These values can be used as guidance with regard to the choice of a proper pillar width for underground twin rock caverns under similar ground conditions.

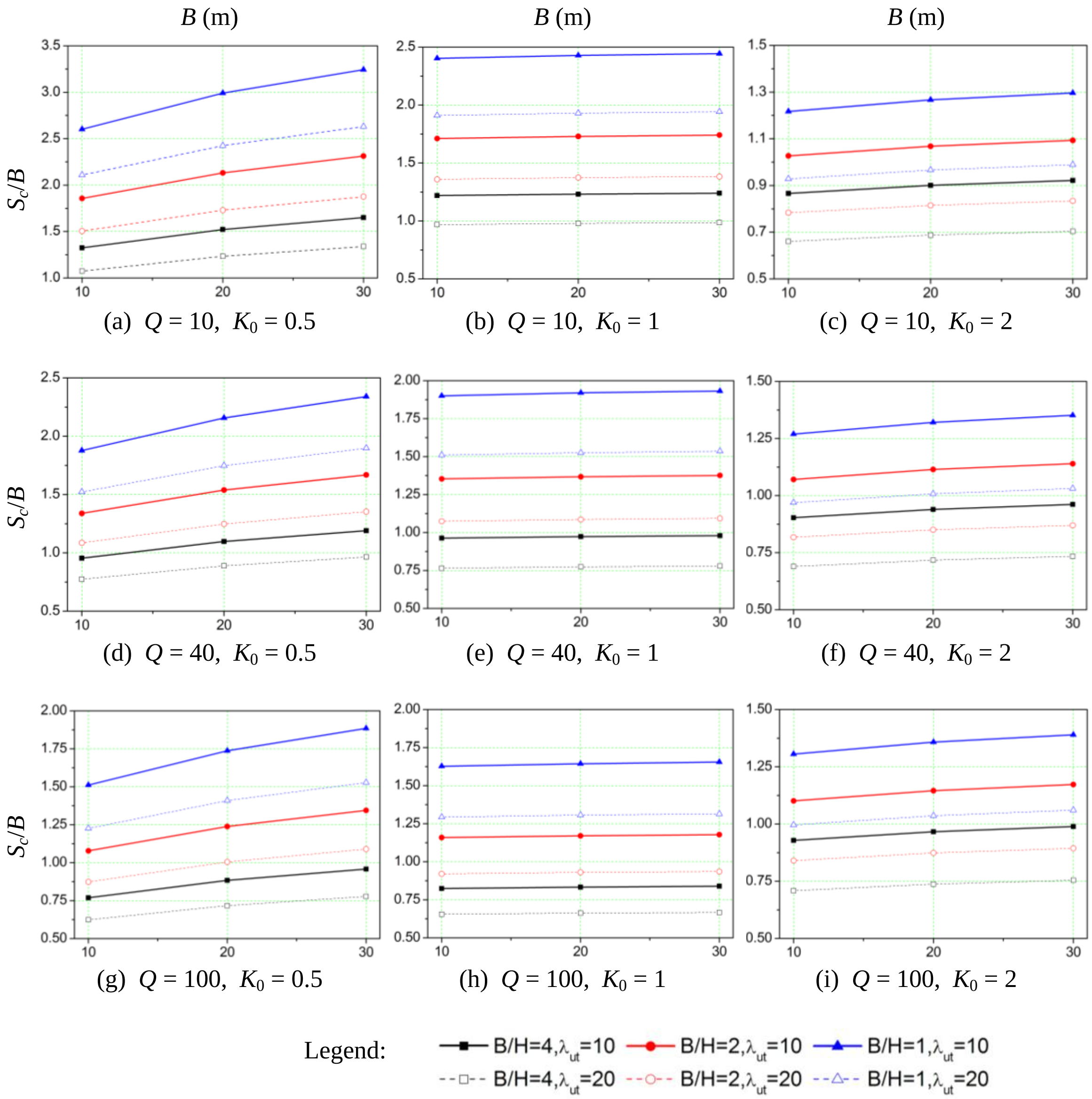

Fig. 6 Design charts for selection of S_c/B based on λ_{ut} = 10 and 20

Table 6 Recommended S_c/B values for λ_{ut} under different conditions

B (m)	B/H	λ_{ut} (%)	Q = 10			Q = 40			Q = 100		
			K_0 = 0.5	K_0 = 1	K_0 = 2	K_0 = 0.5	K_0 = 1	K_0 = 2	K_0 = 0.5	K_0 = 1	K_0 = 2
10	4	10	1.32	1.22	0.75	0.96	0.96	0.72	0.77	0.82	0.70
		20	1.07	0.97	0.57	0.77	0.77	0.55	0.62	0.66	0.54
	2	10	1.86	1.71	0.89	1.34	1.35	0.86	1.08	1.16	0.83
		20	1.50	1.36	0.68	1.09	1.07	0.65	0.87	0.92	0.64
	1	10	2.60	2.40	1.06	1.88	1.89	1.01	1.51	1.63	0.99
		20	2.11	1.91	0.81	1.52	1.51	0.77	1.23	1.29	0.75
20	4	10	1.52	1.23	0.78	1.10	0.97	0.75	0.88	0.83	0.73
		20	1.23	0.98	0.60	0.89	0.77	0.57	0.72	0.66	0.56
	2	10	2.13	1.73	0.93	1.54	1.37	0.89	1.24	1.17	0.87
		20	1.73	1.37	0.71	1.25	1.09	0.68	1.00	0.93	0.66
	1	10	2.99	2.43	1.10	2.16	1.92	1.06	1.74	1.64	1.03
		20	2.42	1.93	0.84	1.75	1.52	0.81	1.41	1.31	0.78
30	4	10	1.65	1.24	0.80	1.19	0.98	0.77	0.96	0.84	0.75
		20	1.34	0.98	0.61	0.96	0.78	0.59	0.78	0.67	0.57
	2	10	2.31	1.74	0.95	1.67	1.38	0.91	1.34	1.18	0.89
		20	1.88	1.38	0.73	1.35	1.09	0.70	1.09	0.94	0.68
	1	10	3.24	2.44	1.13	2.34	1.93	1.08	1.88	1.65	1.05
		20	2.63	1.94	0.86	1.90	1.53	0.82	1.53	1.31	0.80

7. Conclusions

Based on the results of hypothetical cases, this paper presents two LR models used for underground twin rock cavern design, estimating the global factor of safety and the induced maximum displacement, respectively. The concept of Influence Factor λ_{ut} is proposed in this study to quantify the influence of excavation of the second cavern on the existing opening. The LR models developed for predicting λ_{ut} in terms of design parameter are built. The threshold λ_{ut} values can be used to limit the deformation induced as a result of excavation of the adjacent cavern, thus determining a proper S_c/B value. Pillar widths listed in Table 6 are also recommended for general project preliminary use for assessing stability and serviceability requirements under similar ground conditions.

It should be noted that the numerical findings in this study are mainly for preliminary design purposes. For detailed design, extensive laboratory and field testing as well as physical model tests and field instrumentations are essential. It should also be emphasized that the analyses were carried out considering an overburden of 65 m and this study will be extended to take deeper overburdens into account. This study will also continue to investigate the use of other constitutive models such as the Hoek-Brown model instead of Mohr-Coulomb failure criterion, to model the rock mass.

Acknowledgments

The first author would like to thank Prof. Lu Ming for valuable discussions about pillar design.

References

Adoko, A.C., Jiao, Y.Y., Wu, L., Wang, H. and Wang, Z.H. (2013), "Predicting tunnel convergence using Multivariate Adaptive Regression Spline and Artificial Neural Network", *Tunn. Undergr. Space Technol.*, **38**, 368-376.

Barla, G. and Ottoviani, M. (1974), "Stresses and displacements around two adjacent circular openings near to the ground surface", *Proceedings of the 3rd International Congress on Rock Mechanics*, National Academy of Sciences, Denver, CO, USA, September, pp. 975-980.

Basarir, H. (2008), "Analysis of rock-support interaction using numerical and multiple regression modeling", *Can. Geotech. J.*, **45**(1), 1-13.

Bieniawski, Z.T. (1978), "Determining rock mass deformability: experience from case histories", *Int. J. Rock Mech. Min. Sci. Geomech. Abstr.*, **15**(5), 237-247.

Bieniawski, Z.T. (1989), *Engineering Rock Mass Classifications*, John Wiley and Sons, New York, USA.

Dawson, E.M., Roth, W.H. and Drescher, A. (1999), "Slope stability analysis by strength reduction", *Géotechnique*, **49**(6), 835-840.

Dawson, E.M., Motamed, F., Nesarajah, S. and Roth, W.H. (2000), "Geotechnical stability analysis by strength reduction", *Proceedings of Sessions of Geo-Denver 2000-Slope Stability*, **289**, 99-113.

Esterhuizen, G.S., Dolinar, D.R. and Ellenberger, J.L. (2011), "Pillar strength in underground stone mines in the United States", *Int. J. Rock Mech. Min. Sci.*, **48**(1), 42-50.

Gercek, H. (2005), "Interaction between parallel underground openings", *Proceedings of the 19th International Mining Congress and Fair of Turkey*, IMCEV2005, Izmir, Turkey, pp. 73-81.

Ghaboussi, J. and Ranken, R.E. (1977), "Interaction between two parallel tunnels", *Int. J. Numer. Anal. Meth. Geomech.*, **1**(1), 75-103.

Goh, A.T.C. and Zhang, W.G. (2012), "Reliability assessment of stability of underground rock caverns", *Int. J. Rock Mech. Min. Sci.*, **55**, 157-163.

Hammah, R.E., Yacoub, T. and Curran, J.H. (2007), "Serviceability-based slope factor of safety using the shear strength reduction (SSR) method", *Proceedings of the 11th Congress of the International Society for Rock Mechanics*, Lisbon, Portugal, July, pp. 1137-1140.

Jiao, Y.Y., Song, L., Wang, X.Z. and Adoko, A.C. (2013a), "Improvement of the U-shaped steel sets for supporting the roadways in loose coal seam", *Int. J. Rock Mech. Min. Sci.*, **60**, 19-25.

Jiao, Y.Y., Wang, Z.H., Wang, X.Z., Adoko, A.C. and Yang, Z.X. (2013b), "Stability assessment of an ancient landslide crossed by two coal mine tunnels", *Eng. Geol.*, **159**, 36-44.

Jiao, Y.Y., Tian, H.N., Liu, Y.Z., Mei, R.W. and Li, H.B. (2015), "Prediction of tunneling hazardous geological zones using the active seismic approach". *Near Surf. Geophys.*, **13**(4), 333-342.

Karademir, S.M. (2010), "A parametric study on three dimensional modeling of parallel tunnel interactions", Ph.D. Thesis; Middle East Technical University, Ankara, Turkey.

Li, S.J., Feng, X.T. and Li, Z.H. (2012), "Evolution of fractures in the excavation damaged zone of a deeply buried tunnel during TBM construction", *Int. J. Rock Mech. Min. Sci.*, **55**, 125-138.

Lü, Q., Chan, C.L. and Low, B.K. (2012), "Probabilistic evaluation of ground-support interaction for deep rock excavation using artificial neural network and uniform design", *Tunn. Undergr. Space Technol.*, **32**, 1-18.

Mahdevari, S. and Torabi, S.R. (2012), "Prediction of tunnel convergence using Artificial Neural Networks", *Tunn. Undergr. Space Technol.*, **28**, 218-228.

Matsui, T. and San, K.C. (1992), "Finite element slope stability analysis by shear strength reduction technique", *Soil. Found.*, **32**(1), 59-70.

Mortazavi, A., Hassani, F.P. and Shabani, M. (2009), "A numerical investigation of rock pillar failure mechanism in underground openings", *Comput. Geotech.*, **36**(5), 691-697.

Palmstrom, A. (2000), "On classification systems", *Proceedings GeoEng2000,* Melbourne, Australia, November.

Rafiai, H. and Moosavi, M. (2012), "An approximate ANN-based solution for convergence of lined circular tunnels in elasto-plastic rock masses with anisotropic stresses", *Tunn. Undergr. Space Technol.*, **27**(1), 52-59.

Serafim, J.L. and Pereira, J.P. (1983), "Considerations of the geomechanics classification of Bieniawski", *Proceedings of the International Symposium on Engineering Geology and Underground Construction*, Volume 1, Rotterdam, The Netherlands, month, pp. 1133-1142.

Siahmansouri, A., Gholamnejad, J. and Marji, M.F. (2012), "A new method to predict ratio of width to height rock pillar in twin circular tunnels", *J. Geol. Geosci.*, **1**, 103. DOI: 10.4172/2329-6755.1000103

Tugrul, A. (1998), "The application of rock mass classification systems to underground excavation in weak lime stone, Ataturk dam", *Turkey Eng. Geol.*, **50**(3-4), 337-345.

Vermeer, P.A., Ruse, N. and Marcher, T. (2002), "Tunneling heading stability in drained ground", *Felsbau* **20**(6), 8-18.

Zhang, W.G. and Goh, A.T.C. (2012), "Reliability assessment on ultimate and serviceability limit states and determination of critical factor of safety for underground rock caverns", *Tunn. Undergr. Space Technol.*, **32**, 221-230.

Zhang, W.G. and Goh, A.T.C. (2013), "Multivariate adaptive regression splines for analysis of geotechnical engineering systems", *Comput. Geotech.*, **48**, 82-95.

Zhao, B.Y. and Ma, Z.Y. (2009), "Influence of cavern spacing on the stability of large cavern groups in a hydraulic power station", *Int. J. Rock Mech. Min. Sci.*, **46**(3), 506-513.

Zhu, W.S., Sui, B., Li, X.J., Li, S.C. and Wang, W.T. (2008), "A methodology for studying the high wall displacement of large scale underground cavern complexes and its applications", *Tunn. Undergr. Space Technol.*, **23**(6), 651-664.

CC